

Phenomenology of electroweak spin-1 resonances

R. Caliri,^a J. Hadlik,^a M. Kunkel,^a W. Porod^{a,*} and Ch. Verollet^b

^a*Institut für Theoretische Physik und Astrophysik, University of Würzburg,
Emil-Hilb-Weg 22, D-97074 Würzburg, Germany*

^b*Institut de Physique des 2 Infinis de Lyon (IP2I),*

69100 Villeurbanne Cedex, France

E-mail: rosy.caliri@uni-wuerzburg.de, jan.hadlik@uni-wuerzburg.de,

manuel.kunkel@uni-wuerzburg.de, werner.porod@uni-wuerzburg.de,

c.verollet@ip2i.in2p3.fr

Composite Higgs models with a fermionic UV completion predict the existence of various bound states. We investigate models containing $SU(2)_L \times SU(2)_R$ as part of the unbroken global subgroup in the new strong sector. These models predict that there are two neutral and one charged spin-1 resonances mixing seizable with the SM vector bosons. These can be singly produced at the LHC. We explore their LHC phenomenology and demonstrate that there are still viable scenarios consistent with existing LHC data where the masses of these states can be as low as about 1.5 TeV.

Proceedings of the Corfu Summer Institute 2025 "School and Workshops on Elementary Particle Physics and Gravity" (CORFU2025)

27 April - 28 September, 2025

Corfu, Greece

*Speaker

1. Introduction

In composite Higgs models [1, 2] one postulates an additional gauge interaction besides the ones of the Standard Model (SM). These models provide a potential solution to the problem of hierarchy between the electroweak (EW) scale and the Planck scale provided the new interaction become strong in the multi-TeV range leading to the spontaneous breaking of the global symmetries of the new fermions charged under this gauge interaction. The corresponding breaking scale is thus dynamically generated like in quantum chromodynamics (QCD). This breaking should be such, that the Higgs boson emerges as a pseudo Nambu Goldstone boson (pNGBs) [3] and its potential is generated by explicit breaking terms: the gauging of the electroweak symmetry, the couplings of the top quark [4] and a possible mass term for the underlying fermions [5, 6].

The size of the top-mass can be explained via partial compositeness [7] leading to the prediction of top-partners, some of which will mix with the SM quarks of the third generation. In addition, also spin-1 states are predicted, both in the coloured and the electroweak sector. In this contribution, we focus on models based on an underlying gauge-fermion description as they allow for a systematic classification of the properties of the resonances, see ref. [8] for a systematic way to obtain models with the minimal resonances required by the observed Higgs sector. An important class among these models contain two separate species in different irreducible representations (irreps). A set of twelve minimal models, dubbed M1-M12, has been presented in ref. [9, 10].

The proposed models have served as a basis for several phenomenological studies: for electroweak pNGBs see [9, 11–13], for QCD coloured pNGBs [10, 14–16]. Top partners with non-standard decays are discussed in [17–21] and those containing also color octets and sextets in [22, 23]. Spin-1 resonances carrying electroweak charges are discussed in [24, 25] and those with QCD charges in [26]. We note for completeness, that spectra and couplings for such resonances have been computed on the lattice for models based on SU(4) [27–32], e.g. models M6 and M11, and models based on Sp(4) [33–40], e.g. models M5 and M8. Moreover, computations based on holography are also available [41–46]. Both approaches give consistent results for the covered subset of models.

In this contribution we focus on the phenomenology of electroweak charged spin-1 resonances, in particular on those which mix with the SM vector bosons. In the subsequent sections we first summarize relevant model aspects and then focus on LHC phenomenology of the spin-1 resonances. We then discuss to which extent this sector is constrained by existing LHC data in section 4. Finally we conclude with a discussion and an outlook.

2. Model aspects

We summarize here the main aspects and refer to [25] for further details. The so-called vacuum misalignment is characterized by an angle θ which is given by

$$f_\pi \sin \theta = v_{\text{SM}} = 246 \text{ GeV} . \quad (1)$$

with f_π being the decay constant of the pNGBs and v_{SM} is the vacuum expectation value of the SM Higgs boson. The spin-1 resonances emerge as bound states of the new fermions. Their properties emerge from three types of cosets, SU(5)/SO(5), SU(4)/Sp(4), and SU(4)²/SU(4). The resulting

coset/particles	pNGBs			\mathcal{A}_μ			\mathcal{V}_μ		
	$SU(2)^2$	$SU(2)_D$	name	$SU(2)^2$	$SU(2)_D$	name	$SU(2)^2$	$SU(2)_D$	name
SU(4)/Sp(4) in M8-M9	(2,2)	3	φ	(2,2)	3	a_μ	(2,2)	3	\hat{r}_μ
		1	H		1	$\hat{y}_{1\mu}$		1	$\hat{x}_{1\mu}$
	(1,1)	1	η	(1,1)	1	$\hat{y}_{2\mu}$	(3,1)+(1,3)	3	$v_{1\mu}$
							3	$v_{2\mu}$	
SU(5)/SO(5) in M1-M7	(2,2)	3	φ	(2,2)	3	a_μ	(2,2)	3	\hat{r}_μ
		1	H		1	$\hat{y}_{1\mu}$		1	$\hat{x}_{1\mu}$
	(1,1)	1	η	(1,1)	1	$\hat{y}_{2\mu}$	(3,1)+(1,3)	3	$v_{1\mu}$
	(3,3)	5	η_5	(3,3)	5	$\hat{a}_{5\mu}$		3	$v_{2\mu}$
		3	η_3		3	$\hat{a}_{3\mu}$			
	1	η_1		1	$\hat{a}_{1\mu}$				
SU(4) ² /SU(4) in M10-M12	(2,2)	3	φ	(2,2)	3	a_μ	(2,2)	3	\hat{r}_μ
		1	H		1	$\hat{y}_{1\mu}$		1	$\hat{x}_{1\mu}$
	(2,2)	3	ϕ_1	(2,2)	3	\hat{a}_μ	(2,2)	3	r_μ
		1	ϕ_2		1	$\hat{y}_{3\mu}$		1	$\hat{x}_{3\mu}$
	(1,1)	1	η	(1,1)	1	$\hat{y}_{2\mu}$	(1,1)	1	$\hat{x}_{2\mu}$
	(3,1)+(1,3)	3	η_1	(3,1)+(1,3)	3	$b_{1\mu}$	(3,1)+(1,3)	3	$v_{1\mu}$
	3	η_2		3	$b_{2\mu}$		3	$v_{2\mu}$	

Table 1: List of pNGBs, axial vector and vector states for the three cosets. For each particle we give first the $SU(2)^2 \equiv SU(2)_L \times SU(2)_R$ representation, the $SU(2)_D$ representation and the name used for the latter. Moreover, we list in the first column the models from ref. [10] that feature the corresponding coset.

spectrum contains a set of vectors \mathcal{V}^μ as well as a set of axial-vectors \mathcal{A}^μ , which decay respectively into two or three pNGBs¹. The latter property originates from the symmetric nature of the cosets. We give in table 1 the resulting pNGBs and spin-1 resonances. The spin-1 states which do *not* mix with the SM EW vector bosons are indicated by a hat on the corresponding name. Their masses are given by two independent parameters M_V and M_A .

In the following we focus on the cosets $SU(4)/Sp(4)$ and $SU(5)/SO(5)$ as for those we have the same mixing patterns with the SM vector bosons [25] and refer for the details of the third coset to [25]. The W^+ -boson mixes with the states a_μ^+ and a linear combination of $v_{1\mu}^+$ and $v_{2\mu}^+$. We denote the corresponding mass eigenstate by $V_{1\mu}^+$ in the following. In the neutral sector the EW vector bosons mix with a_μ^0 , $v_{1\mu}^0$ and $v_{2\mu}^0$. We denote the mass eigenstates which are dominantly a linear combination of $v_{1\mu}^0$ and $v_{2\mu}^0$ by $V_{1\mu}^0$ and $V_{2\mu}^0$. We note, that the mixing with the axial states a_μ^+ and a_μ^0 vanishes in the limit $\sin \theta \rightarrow 0$.

The corresponding mass matrices are diagonalized by orthogonal rotation matrices which we denote by C and \mathcal{N} for the charged and neutral sectors, respectively:

$$\left(\tilde{W}_\mu^+, a_\mu^+, v_{1\mu}^+, v_{2\mu}^+ \right)^T = C \left(W_\mu^+, A_\mu^+, V_{1\mu}^+, V_{2\mu}^+ \right)^T = CR_\mu^+, \quad (2)$$

$$\left(B_\mu, \tilde{W}_\mu^3, a_\mu^0, v_{1\mu}^0, v_{2\mu}^0 \right)^T = \mathcal{N} \left(A_\mu, Z_\mu, A_\mu^0, V_{1\mu}^0, V_{2\mu}^0 \right)^T = \mathcal{N}R_\mu^0, \quad (3)$$

denoting the mass eigenstate vectors by R_μ^+ and R_μ^0 .

¹This is actually an abuse of language. Only in case of the coset $SU(3) \times SU(3)/SU(3)$ the names 'vector' and 'axial-vector' coincides with the CP properties of the spin-1 resonances.

We now collect the interactions that facilitate either the production or the decay of the heavy spin-1 resonances. We focus on the states V_1^0, V_2^0, V_1^+ that still mix with SM vector bosons even if $\sin\theta \rightarrow 0$. This mixing generates couplings between these spin-1 resonances and SM fermions:

$$\mathcal{L}_{\text{CC}} = \frac{\hat{g}}{\sqrt{2}} \sum_{i,f,f'} C_{1i} \bar{\psi}_f \mathcal{R}_i^+ P_L (V_{\text{CKM}})_{ff'} \psi_{f'} + \text{h.c.}, \quad (4)$$

$$\mathcal{L}_{\text{NC}} = \sum_{i,f} \bar{\psi}_f \mathcal{R}_i^0 \left(g_{Li}^f P_L + g_{Ri}^f P_R \right) \psi_f, \quad (5)$$

$$\text{with } g_{Li}^f = \hat{g} T_f^3 \mathcal{N}_{2i} + \hat{g}' Y_{fL} \mathcal{N}_{1i} \quad \text{and} \quad g_{Ri}^f = \hat{g}' Y_{fR} \mathcal{N}_{1i}. \quad (6)$$

Here T_f^3 is the weak isospin of the fermion f and Y_{fL}, Y_{fR} are the corresponding hypercharges. These couplings give rise to single production as discussed below.

The third generation quarks get an additional contribution from the mixing between the elementary fields and the top partners in models with partial compositeness (PC), which we parametrize as

$$\mathcal{L}_{\text{PC}} = \bar{t} \left(\mathcal{V}_1^0 + \mathcal{V}_2^0 \right) \left(g_{t,L} P_L + g_{t,R} P_R \right) t + \bar{b} \left(\mathcal{V}_1^0 + \mathcal{V}_2^0 \right) \left(g_{b,L} P_L \right) b + g_{tb,L} \bar{t} \mathcal{V}_1^+ P_L b. \quad (7)$$

Due to the small mixing of the bottom quark with its partner the $g_{b,L}$ will be small. Moreover, we assume here for simplicity that the couplings of V_1^0 and V_2^0 are the same. In practice they differ slightly due to the difference in the corresponding entries of \mathcal{N} , which are however small at the numerical level.

The mixing between the spin-1 resonances and the SM vector boson induce couplings of one spin-1 resonance to two electroweak vector bosons which originate from the terms

$$\begin{aligned} \mathcal{L} \supset & -i \left(\hat{g} \tilde{W}^{+\nu} \tilde{W}_\mu^- \partial^\mu \tilde{W}_\nu^3 + \frac{\tilde{g}}{\sqrt{2}} \left((a^{+\nu} v_{1\mu}^- + v_1^{+\nu} a_\mu^-) \partial^\mu a_\nu^0 + (v_1^{+\nu} v_{2\mu}^- + v_2^{+\nu} v_{1\mu}^-) \partial^\mu v_{2\nu}^0 \right) \right. \\ & \left. + \frac{\tilde{g}}{\sqrt{2}} \left(a^{+\nu} a_\mu^- + v_1^{+\nu} v_{1\mu}^- + v_2^{+\nu} v_{2\mu}^- \right) \partial^\mu v_{1\nu}^0 \right) + \text{permutations} . \quad (8) \end{aligned}$$

Moreover, there are couplings of a spin-1 resonance to two pNGBs which is characterized by the vector-pNGB-pNGB coupling constant $g_{V\pi\pi}$ which is the analog of $g_{\rho\pi\pi}$ coupling in QCD. There is a second contribution to this coupling originating from mixing of the spin-1 resonances with the SM vector bosons [25]. Moreover, the spin-1 resonances couple to the Higgs boson and one SM vector boson.

The couplings and mixing matrices are characterized by four parameters: the vector mass parameter M_V , the ratio of axial to vector mass $\xi = M_A/M_V$, the coupling scale of vectors to two pNGBs $g_{V\pi\pi}$ and the decay constant f_π . In addition one has the strong coupling \tilde{g} of the new sector as a free parameter. In the following we will fix the pion decay constant f_π to 1 TeV as its variation only mildly affects the decay channels of interest. Both, lattice studies [30, 34, 35, 39] and holographic models using gauge/gravity duality [41–46] yield $\xi > 1$ and, thus, we set $\xi = 1.4$ in the following. Additionally, we use the SM values of the electric charge e and mass of the Z boson M_Z as input parameters.

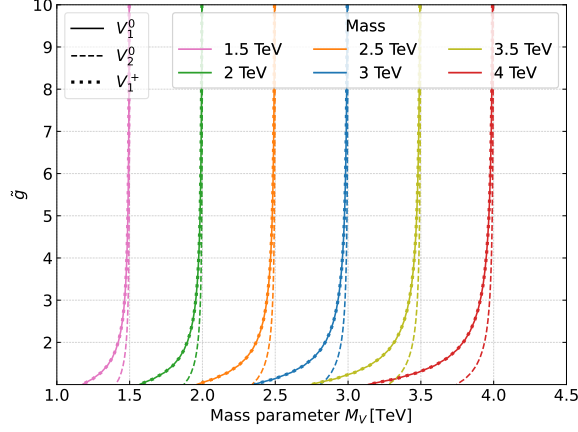


Figure 1: Contour lines for the masses of $V_{1\mu}^+$, $V_{1\mu}^0$ and $V_{2\mu}^0$ in the M_V - \tilde{g} plane. The results look nearly identical for each coset $SU(4)/Sp(4)$, $SU(5)/SO(5)$ and $SU(4) \times SU(4)/SU(4)$.

3. Relevant phenomenological aspects

The states, which mix with the SM electroweak bosons even in the limit $\sin\theta \rightarrow 0$, can be singly produced with a sizeable cross section at the LHC as we will see below. They are denoted as V_1^+ , V_1^0 and V_2^0 . The first two states stem essentially from $(3, 1)$ of $SU(2)_L \times SU(2)_R$ whereas V_2^0 is mainly the neutral state of $(1, 3)$ mixing primarily with the hypercharge boson. This is also visible in fig. 1 where we show corresponding contour lines for the masses of these states in the M_V - \tilde{g} plane. All states are nearly mass degenerate for $\tilde{g} \gtrsim 4$.

We are interested in the bounds on these states from existing LHC. For these considerations, it is useful to group the various decay channels as follows

$$\mathcal{V}^0 \rightarrow q\bar{q}, l^+l^-, \nu\bar{\nu}, \quad \mathcal{V}^0 \rightarrow t\bar{t}, \quad \mathcal{V}^0 \rightarrow \pi\pi, HZ, W^+W^-, \quad (9)$$

$$\mathcal{V}^+ \rightarrow q\bar{q}', l^+\nu, \quad \mathcal{V}^+ \rightarrow t\bar{b}, \quad \mathcal{V}^+ \rightarrow \pi\pi, W^+Z, W^+H. \quad (10)$$

The phenomenology of these states depends on various unknown parameters. Thus, we consider four exemplary scenarios which are characterized by combinations of couplings to pNGBs and the top quark:

$$\mathbf{SM}t : \quad g_{t,L/R} = g_{Ztt,L/R}^{\text{SM}}, \quad g_{b,L} = g_{Zbb,L}^{\text{SM}}, \quad g_{tb,L} = g_{Wtb}^{\text{SM}}, \quad (11)$$

$$\mathbf{PC}t : \quad g_{t,L} = \frac{1}{\sqrt{10}}, \quad g_{t,R} = \frac{3}{\sqrt{10}}, \quad g_{b,L} = \frac{1}{\sqrt{10}}, \quad g_{tb,L} = \frac{1}{\sqrt{5}}. \quad (12)$$

For the pNGB couplings we consider

$$\mathbf{weak} \pi : \quad g_{V\pi\pi} = 0, \quad (13)$$

$$\mathbf{strong} \pi : \quad g_{V\pi\pi} = 4. \quad (14)$$

We show in fig. 2 the partial decay widths for the various scenarios. For the $SU(4)/Sp(4)$ coset, the black lines representing the decays into the additional pNGBs are absent as there is no coupling of the gauge singlet η to any combination of the electroweak vector bosons and any of

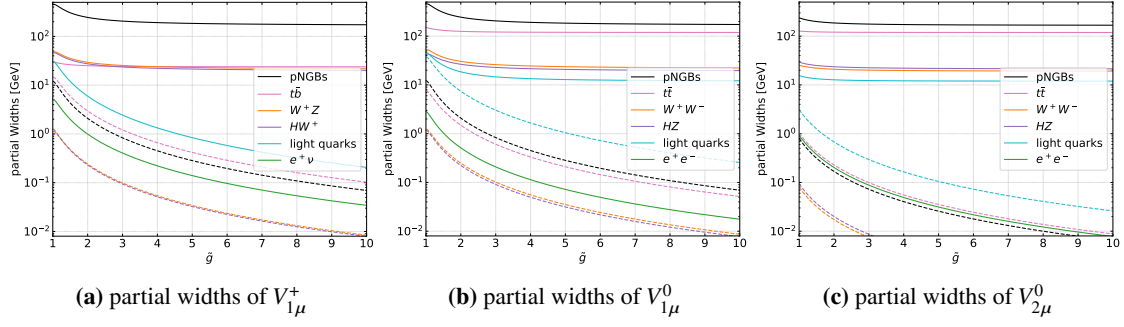


Figure 2: Partial decay widths of selected spin-1 resonances for the SU(5)/SO(5) coset. We have set $M_V = 3000$ GeV and $M_\pi = 700$ GeV. pNGB, W^+W^- , HZ , W^+Z and HW^+ channels: the solid lines of the correspond to $g_{V\pi\pi} = 4$ and the dashed lines correspond to $g_{V\pi\pi} = 0$. Top quark channels: the solid lines correspond to $g_t = 1$ and the dashed lines to SM-like couplings. These also represent the partial widths for the SU(4)/Sp(4) coset for which, however, the black lines (additional pNGB channels) are absent.

the considered spin-1 resonances. We have set the pNGB mass to 700 GeV such that existing LHC bounds are satisfied [12] and $M_V = 3$ TeV. We show the widths for the decays into two bosons for the cases $g_{V\pi\pi} = 4$ and 0 as solid and dashed lines, respectively. Similarly, for the top quark channel we distinguish the PC t and the SM t scenarios by solid and dashed lines. Important features to be observed:

- **PC t , strong π :** In scenarios with large $g_{V\pi\pi}$ and large couplings to top-quarks the spin-1 resonances decay dominantly into the additional pNGBs and $t\bar{t}$ followed by decays into HV and WV ($V = Z, W$) in case the SU(5)/SO(5) coset is realized. In case of the SU(4)/Sp(4) coset, the dominant channel will be $t\bar{t}$ followed by HV and WV . The enhancement of the HV channel is due to the longitudinal components of the vector bosons.
- **PC t , weak π :** In scenarios with large additional top Yukawa couplings and $g_{V\pi\pi} \lesssim O(0.1)$, the $t\bar{t}$ channel dominate independent of the coset.
- **SM t , strong π :** for large $g_{V\pi\pi}$ couplings and SM-like couplings to top quarks, the decays into the additional pNGBs dominate followed by the HV and WV channels in case of the SU(5)/SO(5) coset whereas the latter two channel dominate in case of SU(4)/Sp(4).
- **SM t , weak π :** In case that all additional couplings are small, the decay patterns are similar to those of W and Z bosons but for the additional decays into top quarks. In case of SU(5)/SO(5), the decays into the additional pNGBs are rather important.

These observations imply that we have to take into account the cascade decays via intermediate pNGBs. Here we summarize the various possibilities and refer to the literature for further details [9, 11, 12]. We assume in the following that none of the additional states mixes with the Higgs boson. We denote here the additional states generically as S^0 , S^+ and S^{++} depending on their charge.

As one limiting case we consider the case that the pNGBs decay dominantly into third generation quarks in all cosets and dub this the fermiophilic scenario below. These decays are mainly induced by the mixing of the top and bottom quarks with the top-partners. The neutral states S^0 decay as

$$S_i^0 \rightarrow t\bar{t}, \quad b\bar{b} \quad (15)$$

with the $b\bar{b}$ channel being suppressed by the ratio $(m_b/m_t)^2$. Similarly, S^+ decays as

$$S^+ \rightarrow t\bar{b}. \quad (16)$$

The coset SU(5)/SO(5) features a doubly charged scalar which decays as

$$S^{++} \rightarrow W^+t\bar{b} \quad (17)$$

via an intermediate S^+ [12].

In case that these pNGB couplings to quarks are absent – dubbed fermiophobic scenario –, decays into two SM vector bosons induced by the anomalous WZW terms are relevant. Cascade decays into a vector boson and another pNGB are also important in scenarios with a mass splitting between the pNGBs [12]. We take here the SU(5)/SO(5) coset as a prototypical example where all pNGBs but η_3^0 have anomaly induced couplings. In scenarios in which the triplet is the lightest state of in scenarios with mass degenerate additional pNGBs, which we assume in the following, the CP-even η_3^0 undergoes only three-body decays via an off-shell pNGB:

$$\eta_3^0 \rightarrow W^\mp \eta_{3,5}^\pm \rightarrow W^+W^-\gamma, W^+W^-Z \quad (18)$$

$$\eta_3^0 \rightarrow Z\eta_{1,5}^0 \rightarrow ZZZ, ZZ\gamma, Z\gamma\gamma. \quad (19)$$

Their analytic expressions of the corresponding partial widths are given in [25].

4. Constraints due to existing LHC data

The states V_1^+ and $V_{1,2}^0$ have sizeable couplings to quarks of the first two generations due to the mixing of these states with the SM vector bosons. Thus, they can be singly produced at the LHC as exemplary shown in fig. 3 for the two cosets considered. The various decay modes of the spin-1 resonances discussed above lead to multiple signatures that have been searched for at the LHC. In particular the following searches are relevant to constrain the parameter space of our models considered:

- an ATLAS search for $Z' \rightarrow \ell^+\ell^-$ using 139 fb^{-1} [47],
- an ATLAS search for $Z' \rightarrow t\bar{t}$ using 139 fb^{-1} [48],
- an ATLAS search for $W' \rightarrow \ell^+\nu$ using 139 fb^{-1} [49],
- an ATLAS search for $W' \rightarrow t\bar{b}$ using 139 fb^{-1} [50].

To this end, all relevant vertices have been implemented in the FeynRules [51] format to obtain an UFO library [52]. This UFO has been used to generate events of the respective process at $\sqrt{s} = 13 \text{ TeV}$ with MadGraph5_aMC@NLO [53] v3.5.3. Dynamical renormalization and factorization scales have been used together with the NNPDF 2.3 set of parton distribution functions [54] implemented in LHAPDF [55]. This has been used to calculate the cross sections of a given process for a grid of parameter points, which are compared to the upper limits obtained from the above listed searches to derive exclusion limits in the M_V - \tilde{g} -plane.

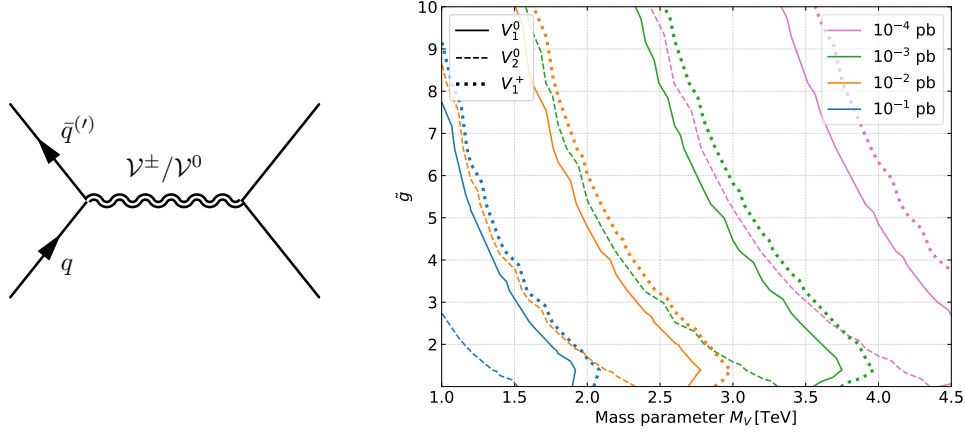


Figure 3: Drell-Yan production of heavy vectors. To the left: typical Feynman diagrams. To the right: production cross sections at $\sqrt{s} = 13$ TeV of the heavy vector states in the M_V - \tilde{g} -plane for a small $g_{V\pi\pi}$ coupling and nearly SM-like couplings to top-quarks. The cross sections are the same for both cosets, SU(5)/SO(5) and SU(4)/Sp(4).

We have recast searches for final states with two bosons as they are not covered by any experimental search. To this end, we have first showered and hadronized the events with Pythia8 [56] to produce a HepMC file [57]. The hadronized events have passed to MadAnalysis5 [58–61] v1.10.9beta and CheckMATE [62, 63] commit number 1cb3f7. Both tools cluster the jets with the anti- k_T algorithm [64] implemented in the FastJet library [65] and simulate the detector response with Delphes 3 [66]. These events have then been run through the kinematic cuts of the recast searches, and from the number of remaining events an exclusion value has been calculated with the CL_s method [67] for every signal region. We have collected the observed exclusion for the signal region for every search that had the strongest expected bound. In addition, we have run the events against the SM measurements implemented in Rivet [68] v3.1.8 and we have evaluated the results with Contur [69] v2.4.4. We report the strongest exclusion from any individual search as final result. Note, that we have not performed any statistical combination beyond what is implemented in these tools. From this we have obtained contours of the exclusion at 95% CL as bound in the M_V - \tilde{g} -plane. We note for completeness, that the regions with small $\tilde{g} \lesssim 2$ are not entirely reliable for the scenarios with strong pNGB coupling as the widths of the vector resonances $V_{1\mu}^{0,\pm}$ exceed 10% of their respective mass.

We show in fig. 4 the resulting bounds are shown in for the coset SU(5)/SO(5) as an example and refer to [25] for the other two. Note, that the x-axis is not the physical mass of the vectors but the mass parameter M_V . We see in figs. 4a and 4b, that strong bounds are obtained if both the couplings to top quarks and pNGBs are small, leaving a sizable branching ratio for decays into leptons. In the other three scenarios the bounds are similar to each other. The bounds from $V^\pm \rightarrow t\bar{b}$ are significantly stronger compared to the bounds from the decays of the neutral resonances into $t\bar{t}$, see figs. 4c and 4d, due to the increased cross section of the charged channel.

We show the bounds from decays into pNGBs in the fermiophilic (solid lines) and fermiophobic (dotted lines) scenarios in fig. 4e. The latter are strongly constrained by the recast of ref. [70], a search for photonic signatures of supersymmetry implemented in CheckMATE. The bounds are

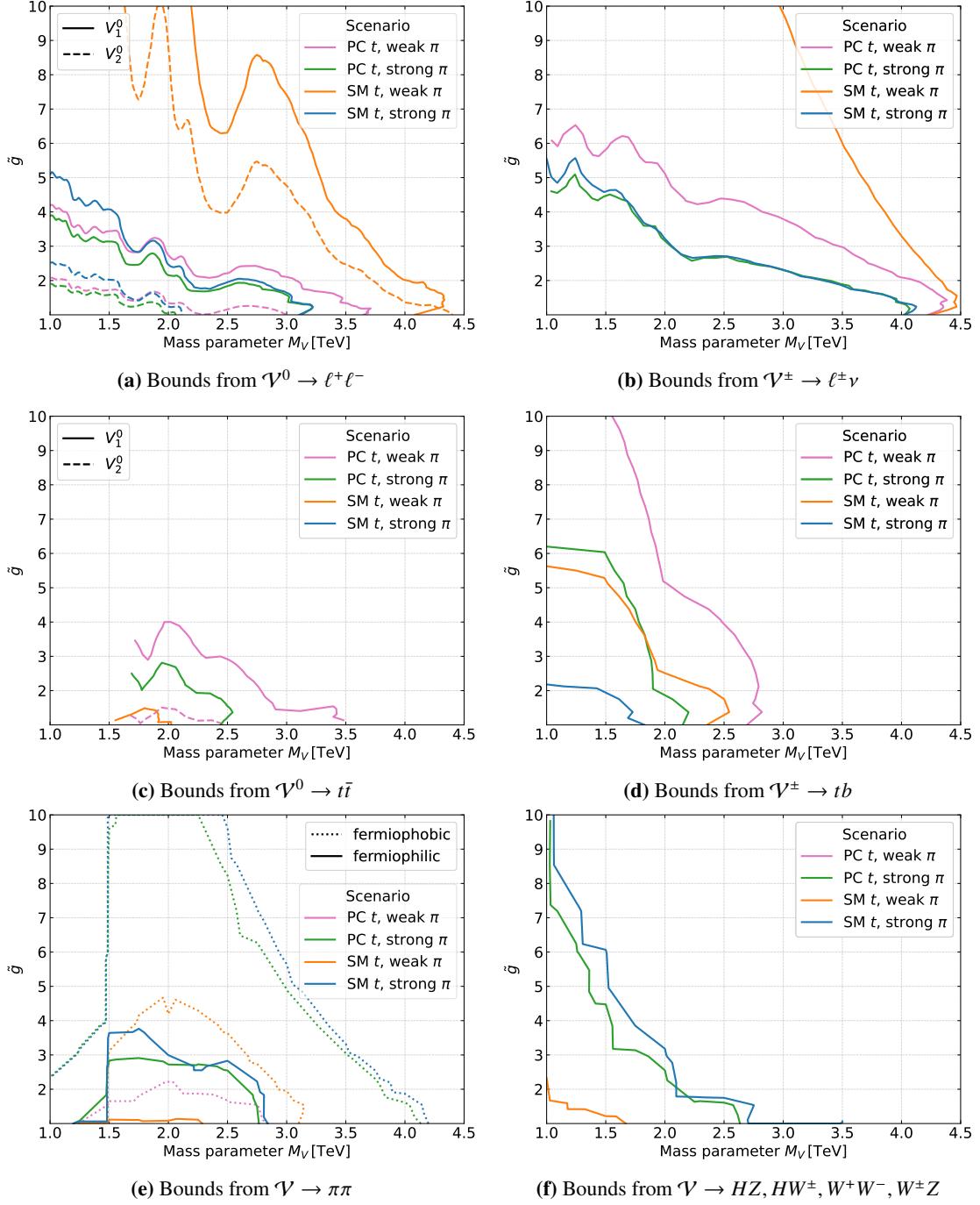


Figure 4: Bounds on the single production of heavy spin-1 resonances in the $SU(5)/SO(5)$ coset for a pNGB mass of 700 GeV. In the scenarios, “SM t ” means the couplings of the $\mathcal{V}^0/\mathcal{V}^\pm$ to $t\bar{t}/tb$ are given as in eq. 11 whereas for “PC t ” they are set to the values in eq. 12. In case of pNGBs, “weak” and “strong π ” refers to $g_{V\pi\pi} = 0$ and $g_{V\pi\pi} = 4$, respectively. In plots (a)-(d) the upper limits on the cross sections are obtained from direct searches [47–50]. In plot (e) we distinguish between fermiophobic and fermiophilic scenarios of the pNGBs as discussed in the text. The bounds are derived from recasts of [70] and [71–74], respectively. The bounds in plot (f) are derived from recasts of [75–86]. The regions with small $\tilde{g} \lesssim 2$ have to be taken with a grain of salt for scenarios with strong π since the resonances are no longer narrow.

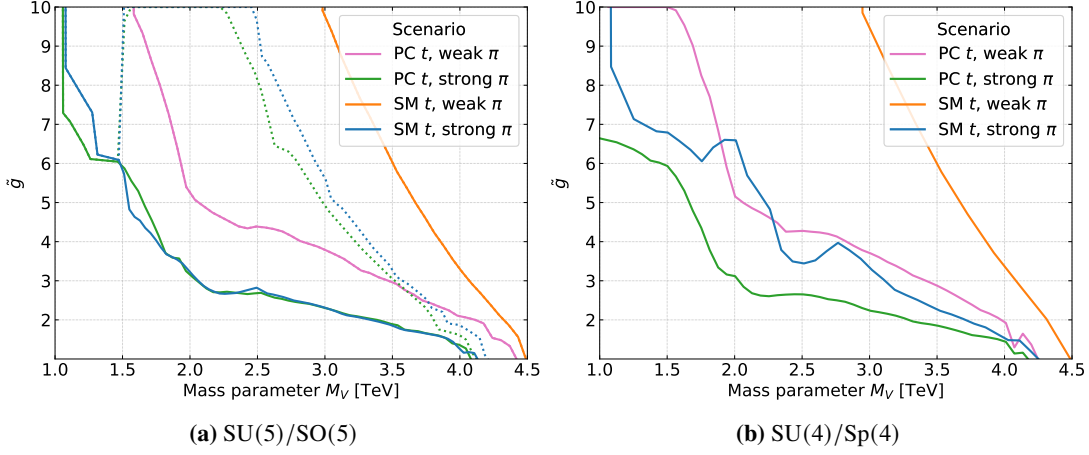


Figure 5: Left: bounds on the single production of heavy vectors in the $SU(5)/SO(5)$ coset. For each scenario we show the envelope of the bounds from the individual channels shown in fig. 4, i.e. the strongest bound at every point. The solid lines correspond to the fermiophilic, the dotted lines to the fermiophobic model, both with $M_\pi = 700$ GeV. Right: corresponding bounds for the $SU(4)/Sp(4)$ coset for a pNGB masses of $M_\pi = 450$ GeV.

derived for a common pNGB mass $M_\pi = 700$ GeV to evade constraints from Drell-Yan production of pNGBs [12]. The sudden drop of the exclusion lines at $M_V \approx 2M_\pi$ is due to kinematic suppression of the pNGB channels. The bounds on pNGB decays into quarks are considerably weaker. In figure 4f we show the bounds derived from decays into two gauge bosons or one gauge and one Higgs boson. For small masses, these channels dominate in the strong π scenarios, but get strongly suppressed above the threshold for pNGB pair production.

The individual channels need to be combined to get the resulting bound on the underlying parameter space. We show in fig. 5a the combined bounds for all four coupling scenarios where each line represents the envelope of all channels. In the two scenarios with strong coupling to the pNGBs we show the fermiophilic scenario as a solid line and indicate where the fermiophobic case differs by a dotted line. The scenario with weak couplings to top and pNGBs (orange line) is strongly constrained yielding $M_V > 3$ TeV – 4.5 TeV depending on \tilde{g} . The bounds are considerably weaker, with M_V down to 2 TeV remaining viable with only moderate \tilde{g} provided only the PC couplings are turned on (pink line). The fermiophobic scenario is more strongly constrained than the fermiophilic one. The scenario with large $g_{V\pi\pi}$ and SM like couplings to the top-quarks leaves the largest part of parameter space open, in particular in the fermiophilic case. The corresponding results for the $SU(4)/Sp(4)$ coset are shown in fig. 5b. It differs only in the pNGB sector which features significantly less states as can be seen from table 1. Again, in particular the scenario with no enhancement for the couplings to top quarks and pNGBs is strongly constrained.

5. Conclusions and outlook

We have investigated the phenomenology of electroweak spin-1 resonances in Composite Higgs Models paying particular attention to bounds from existing LHC data. The focus has been on models with gauge fermionic UV completions [9, 10] because they provide detailed information

on the quantum numbers and properties of the bound states. More precisely, we have considered the cosets $SU(4)/Sp(4)$ and $SU(5)/SO(5)$. In view of the LHC phenomenology, the states which can mix with the electroweak vector bosons of the SM are the most constraint ones as they can be singly produced. Independent of the coset there is always one charged spin-1 resonance mixing sizably with the W-boson and two neutral spin-1 resonances mixing sizably with the Z-boson. This is a consequence of the fact that in all cases the unbroken subgroup contains the custodial group $SU(2)_L \times SU(2)_R$ by construction.

We have used various analyses to obtain bounds in the mass-coupling plane for these states. Direct searches for heavy resonances in the s-channel at the LHC are used for decays of the spin-1 resonances into two SM fermions. In addition we have used recast searches for final states containing two bosons, either pNGBs and/or SM vector bosons as for these no direct searches had been performed. We have investigated four different cases to study the effect of unknown model dependent couplings. We have found, masses as low as 1.5 TeV are still allowed by current LHC data in scenarios with sizeable couplings of the spin-1 resonances to pNGBs. In this part of the parameter space, also the states which only mix weakly or not at all will have masses in the same range.

One might get further bounds or even discover these in processes such as

$$gg \rightarrow b\bar{b}V^0, t\bar{t}V^0 \quad (20)$$

$$gg \rightarrow b\bar{t}V^+, t\bar{b}V^- . \quad (21)$$

Moreover, a projective future circular collider [87–89] will offer additional possibilities for the pair production of these states.

Acknowledgements

We thank the organizers of the workshop for provided such an stimulating environment. This work has been supported by DFG, project no. PO-1337/12-1 as well as the research training group GRK-2994.

References

- [1] D. B. Kaplan and H. Georgi, *Phys. Lett. B* **136** (1984), 183-186.
- [2] D. B. Kaplan, H. Georgi and S. Dimopoulos, *Phys. Lett. B* **136** (1984), 187-190.
- [3] R. Contino, Y. Nomura and A. Pomarol, *Nucl. Phys. B* **671** (2003), 148-174 [arXiv:hep-ph/0306259 [hep-ph]].
- [4] K. Agashe, R. Contino and A. Pomarol, *Nucl. Phys. B* **719** (2005), 165-187 [arXiv:hep-ph/0412089 [hep-ph]].
- [5] J. Galloway *et al.*, *JHEP* **10** (2010), 086 [arXiv:1001.1361 [hep-ph]].
- [6] G. Cacciapaglia and F. Sannino, *JHEP* **04** (2014), 111 [arXiv:1402.0233 [hep-ph]].

- [7] D. B. Kaplan, *Nucl. Phys. B* **365** (1991), 259-278.
- [8] G. Ferretti and D. Karateev, *JHEP* **03** (2014), 077 [arXiv:1312.5330 [hep-ph]].
- [9] G. Ferretti, *JHEP* **06** (2016), 107 [arXiv:1604.06467 [hep-ph]].
- [10] A. Belyaev *et al.*, *JHEP* **01** (2017), 094 [erratum: *JHEP* **12** (2017), 088] [arXiv:1610.06591 [hep-ph]].
- [11] A. Agugliaro *et al.*, *JHEP* **02** (2019), 089 [arXiv:1808.10175 [hep-ph]].
- [12] G. Cacciapaglia *et al.*, *JHEP* **12** (2022), 087 [arXiv:2210.01826 [hep-ph]].
- [13] T. Flacke *et al.*, *JHEP* **11** (2023), 009 [arXiv:2304.09195 [hep-ph]].
- [14] G. Cacciapaglia *et al.*, *JHEP* **11** (2015), 201 [arXiv:1507.02283 [hep-ph]].
- [15] G. Cacciapaglia *et al.*, *JHEP* **05** (2020), 027 [arXiv:2002.01474 [hep-ph]].
- [16] T. Flacke *et al.*, *JHEP* **02** (2026), 028 [arXiv:2506.04318 [hep-ph]].
- [17] N. Bizot, G. Cacciapaglia and T. Flacke, *JHEP* **06** (2018), 065 [arXiv:1803.00021 [hep-ph]].
- [18] K. P. Xie, G. Cacciapaglia and T. Flacke, *JHEP* **10** (2019), 134 [arXiv:1907.05894 [hep-ph]].
- [19] G. Cacciapaglia *et al.*, *Phys. Lett. B* **798** (2019), 135015 [arXiv:1908.07524 [hep-ph]].
- [20] A. Banerjee, D. B. Franzosi and G. Ferretti, *JHEP* **03** (2022), 200 [arXiv:2202.00037 [hep-ph]].
- [21] A. Banerjee *et al.*, *SciPost Phys. Core* **7** (2024), 079 [arXiv:2406.09193 [hep-ph]].
- [22] G. Cacciapaglia *et al.*, *JHEP* **02** (2022), 208 [arXiv:2112.00019 [hep-ph]].
- [23] G. Cacciapaglia *et al.*, [arXiv:2605.04143 [hep-ph]].
- [24] D. Buarque Franzosi *et al.*, *JHEP* **11** (2016), 076 [arXiv:1605.01363 [hep-ph]].
- [25] R. Caliri *et al.*, *JHEP* **04** (2025), 160 [arXiv:2412.08720 [hep-ph]].
- [26] G. Cacciapaglia *et al.*, *JHEP* **06** (2024), 092 [arXiv:2404.02198 [hep-ph]].
- [27] V. Ayyar *et al.*, *Phys. Rev. D* **97** (2018) no.7, 074505 [arXiv:1710.00806 [hep-lat]].
- [28] V. Ayyar *et al.*, *Phys. Rev. D* **99** (2019) no.9, 094502 [arXiv:1812.02727 [hep-ph]].
- [29] V. Ayyar *et al.*, *Phys. Rev. D* **97** (2018) no.11, 114502 [arXiv:1802.09644 [hep-lat]].
- [30] V. Ayyar *et al.*, *Phys. Rev. D* **97** (2018) no.11, 114505 [arXiv:1801.05809 [hep-ph]].
- [31] V. Ayyar *et al.*, *Phys. Rev. D* **99** (2019) no.9, 094504 [arXiv:1903.02535 [hep-lat]].
- [32] A. Hasenfratz *et al.*, *Phys. Rev. D* **107** (2023) no.11, 114504 [arXiv:2304.11729 [hep-lat]].

- [33] E. Bennett *et al.*, *JHEP* **03** (2018), 185 [arXiv:1712.04220 [hep-lat]].
- [34] E. Bennett *et al.*, *Phys. Rev. D* **101** (2020) no.7, 074516 [arXiv:1912.06505 [hep-lat]].
- [35] E. Bennett *et al.*, *JHEP* **12** (2019), 053 [arXiv:1909.12662 [hep-lat]].
- [36] E. Bennett *et al.*, *Phys. Rev. D* **106** (2022) no.1, 014501 [arXiv:2202.05516 [hep-lat]].
- [37] S. Kulkarni *et al.*, *SciPost Phys.* **14** (2023) no.3, 044 [arXiv:2202.05191 [hep-ph]].
- [38] E. Bennett *et al.*, *Phys. Rev. D* **109** (2024) no.9, 094512 [arXiv:2311.14663 [hep-lat]].
- [39] E. Bennett *et al.*, *Phys. Rev. D* **109** (2024) no.9, 094517 [arXiv:2312.08465 [hep-lat]].
- [40] E. Bennett *et al.*, *Phys. Rev. D* **111** (2025) no.7, 074511 [arXiv:2412.01170 [hep-lat]].
- [41] J. Erdmenger *et al.*, *Phys. Rev. Lett.* **126** (2021) no.7, 071602 [arXiv:2009.10737 [hep-ph]].
- [42] J. Erdmenger *et al.*, *JHEP* **02** (2021), 058 [arXiv:2010.10279 [hep-ph]].
- [43] D. Elander *et al.*, *JHEP* **03** (2021), 182 [arXiv:2011.03003 [hep-ph]].
- [44] D. Elander *et al.*, *JHEP* **05** (2022), 066 [arXiv:2112.14740 [hep-ph]].
- [45] J. Erdmenger *et al.*, *Universe* **9** (2023) no.6, 289 [arXiv:2304.09190 [hep-th]].
- [46] J. Erdmenger *et al.*, *JHEP* **07** (2024), 169 [arXiv:2404.14480 [hep-ph]].
- [47] G. Aad *et al.* [ATLAS], *Phys. Lett. B* **796** (2019), 68-87 [arXiv:1903.06248 [hep-ex]].
- [48] G. Aad *et al.* [ATLAS], *JHEP* **10** (2020), 061 [arXiv:2005.05138 [hep-ex]].
- [49] G. Aad *et al.* [ATLAS], *Phys. Rev. D* **100** (2019) no.5, 052013 [arXiv:1906.05609 [hep-ex]].
- [50] G. Aad *et al.* [ATLAS], *JHEP* **12** (2023), 073 [arXiv:2308.08521 [hep-ex]].
- [51] A. Alloul *et al.*, *Comput. Phys. Commun.* **185** (2014), 2250-2300 [arXiv:1310.1921 [hep-ph]].
- [52] C. Degrande *et al.*, *Comput. Phys. Commun.* **183** (2012), 1201-1214 [arXiv:1108.2040 [hep-ph]].
- [53] J. Alwall *et al.*, *JHEP* **07** (2014), 079 [arXiv:1405.0301 [hep-ph]].
- [54] R. D. Ball *et al.*, *Nucl. Phys. B* **867** (2013), 244-289 [arXiv:1207.1303 [hep-ph]].
- [55] A. Buckley *et al.*, *Eur. Phys. J. C* **75** (2015), 132 [arXiv:1412.7420 [hep-ph]].
- [56] T. Sjöstrand *et al.*, *Comput. Phys. Commun.* **191** (2015), 159-177 [arXiv:1410.3012 [hep-ph]].
- [57] M. Dobbs and J. B. Hansen, *Comput. Phys. Commun.* **134** (2001), 41-46.
- [58] E. Conte, B. Fuks and G. Serret, *Comput. Phys. Commun.* **184** (2013), 222-256 [arXiv:1206.1599 [hep-ph]].

- [59] E. Conte *et al.*, *Eur. Phys. J. C* **74** (2014) no.10, 3103 [arXiv:1405.3982 [hep-ph]].
- [60] B. Dumont *et al.*, *Eur. Phys. J. C* **75** (2015) no.2, 56 [arXiv:1407.3278 [hep-ph]].
- [61] E. Conte and B. Fuks, *Int. J. Mod. Phys. A* **33** (2018) no.28, 18300270 [arXiv:1808.00480 [hep-ph]].
- [62] M. Drees *et al.*, *Comput. Phys. Commun.* **187** (2015), 227-265 [arXiv:1312.2591 [hep-ph]].
- [63] D. Dercks *et al.*, *Comput. Phys. Commun.* **221** (2017), 383-418 [arXiv:1611.09856 [hep-ph]].
- [64] M. Cacciari, G. P. Salam and G. Soyez, *JHEP* **04** (2008), 063 [arXiv:0802.1189 [hep-ph]].
- [65] M. Cacciari, G. P. Salam and G. Soyez, *Eur. Phys. J. C* **72** (2012), 1896 [arXiv:1111.6097 [hep-ph]].
- [66] J. de Favereau *et al.* [DELPHES 3], *JHEP* **02** (2014), 057 [arXiv:1307.6346 [hep-ex]].
- [67] A. L. Read, *J. Phys. G* **28** (2002), 2693-2704.
- [68] C. Bierlich *et al.* *SciPost Phys.* **8** (2020), 026 [arXiv:1912.05451 [hep-ph]].
- [69] A. Buckley *et al.* [CONTUR], *SciPost Phys. Core* **4** (2021), 013 [arXiv:2102.04377 [hep-ph]].
- [70] M. Aaboud *et al.* [ATLAS], *Phys. Rev. D* **97** (2018) no.9, 092006 [arXiv:1802.03158 [hep-ex]].
- [71] G. Aad *et al.* [ATLAS], *Eur. Phys. J. C* **81** (2021) no.7, 600 [erratum: *Eur. Phys. J. C* **81** (2021) no.10, 956] [arXiv:2101.01629 [hep-ex]].
- [72] G. Aad *et al.* [ATLAS], *Eur. Phys. J. C* **81** (2021) no.11, 1023 [arXiv:2106.09609 [hep-ex]].
- [73] CMS coll., *JHEP* **10** (2019), 244 [arXiv:1908.04722 [hep-ex]].
- [74] A. M. Sirunyan *et al.* [CMS], *Phys. Rev. D* **96** (2017) no.3, 032003 [arXiv:1704.07781 [hep-ex]].
- [75] A. M. Sirunyan *et al.* [CMS], *JHEP* **03** (2018), 166 [arXiv:1709.05406 [hep-ex]].
- [76] CMS coll., [CMS-PAS-SUS-19-006](#).
- [77] M. Mrowietz, S. Bein and J. Sonneveld, *Mod. Phys. Lett. A* **36** (2021) no.01, 2141007
- [78] CMS coll., [CMS-PAS-EXO-19-002](#).
- [79] E. Conte and R. Ducrocq, *Mod. Phys. Lett. A* **36** (2021) no.01, 2141012.
- [80] A. M. Sirunyan *et al.* [CMS], *Phys. Rev. Lett.* **124** (2020) no.4, 041803 [arXiv:1910.01185 [hep-ex]].
- [81] ATLAS coll., [ATLAS-CONF-2020-048](#).
- [82] G. Aad *et al.* [ATLAS], *JHEP* **06** (2023), 080 [arXiv:2205.02597 [hep-ex]].

- [83] G. Aad *et al.* [ATLAS], *JHEP* **06** (2021), 003 [arXiv:2103.10319 [hep-ex]].
- [84] A. Tumasyan *et al.* [CMS], *Eur. Phys. J. C* **83** (2023) no.7, 628 [arXiv:2205.04897 [hep-ex]].
- [85] G. Aad *et al.* [ATLAS], *Eur. Phys. J. C* **80** (2020) no.7, 616 [arXiv:1912.02844 [hep-ex]].
- [86] M. Aaboud *et al.* [ATLAS], *Eur. Phys. J. C* **79** (2019) no.10, 884 [arXiv:1905.04242 [hep-ex]].
- [87] M. Benedikt *et al.* [FCC], *Eur. Phys. J. C* **85** (2025) no.12, 1468 [arXiv:2505.00272 [hep-ex]].
- [88] M. Benedikt *et al.* [FCC], *Eur. Phys. J. ST* **234** (2025) no.19, 5713-6197 [arXiv:2505.00274 [physics.acc-ph]].
- [89] M. Benedikt *et al.* [FCC], *Eur. Phys. J. ST* **234** (2025) no.17, 5113-5383 [erratum: *Eur. Phys. J. ST* **234** (2025), 33-44] [arXiv:2505.00273 [physics.acc-ph]].